

Shell models and the possibility of application to fusion plasmas

This article has been downloaded from IOPscience. Please scroll down to see the full text article.

2010 Plasma Phys. Control. Fusion 52 045002

(<http://iopscience.iop.org/0741-3335/52/4/045002>)

View [the table of contents for this issue](#), or go to the [journal homepage](#) for more

Download details:

IP Address: 137.110.33.253

The article was downloaded on 31/05/2013 at 21:08

Please note that [terms and conditions apply](#).

Shell models and the possibility of application to fusion plasmas

Ö D Gürçan¹, P Hennequin¹, L Vermare¹, X Garbet² and P H Diamond³

¹ Laboratoire de Physique des Plasmas, Ecole Polytechnique, CNRS, 91128 Palaiseau Cedex, France

² CEA, IRFM, F-13108 Saint Paul Lez Durance, France

³ Center for Astrophysics and Space Sciences, University of California San Diego, 9500 Gilman Dr., CA 92093-0424, USA

Received 25 September 2009, in final form 21 December 2009

Published 5 March 2010

Online at stacks.iop.org/PPCF/52/045002

Abstract

An extensive study of spectral shell models with possibilities for application to fusion plasmas is discussed. A set of shell models addressing various aspects of the characteristics of fusion plasmas have been derived. Difficulties associated with plasma medium, namely its intrinsic excitability, and importance of mescales have been discussed. The numerical implementation of shell models is discussed. It was observed that depending on the parameter regime, they may lead to steady state or display characteristics of predator–prey dynamics.

(Some figures in this article are in colour only in the electronic version)

1. Introduction

1.1. Background

Plasma micro-turbulence plays a crucial role in today's fusion devices since the transport in these devices is dominated by turbulent processes. It is well known that there are certain similarities between neutral fluid turbulence and plasma turbulence. It is also known that certain simplifying assumptions regularly invoked in the theoretical studies of fluid turbulence, such as isotropy, homogeneity and the locality of the cascade processes, are indeed incompatible with plasma turbulence. Nevertheless, various statistical methods developed for describing fluid turbulence are used also for plasma turbulence. Likewise, physical insight obtained from studying fluid turbulence is widely applied to understanding plasma turbulence. In some cases, where the similarity is of an essential nature, such insight is invaluable as it provides a simple understanding of the behavior of a complex system. In other cases, where the differences are more essential, the insight from fluid turbulence is only of marginal utility.

Turbulence spectrum in plasma turbulence is generally accepted to be an important measure. It is important, first and foremost, because it can be measured directly [1–4], and computed in numerical simulations [5–7], where detailed theories exist, that link the

quasi-linear spectrum to the balance between linear growth and Compton scattering [8, 9]. Fluctuation spectrum readily contains the information leading to turbulent diffusion (e.g. χ_i , the turbulent heat diffusivity) under reasonable assumptions, providing, in addition, a description of scales that contribute to this transport. It is commonly invoked as part of the validation metric in the context of validation and verification studies [10]. It is also one of the few quantities for which detailed theories predicting power law solutions exist in neutral fluids [11].

Common wisdom from fluid turbulence suggests that a power law turbulence spectrum in an ‘inertial range’—defined in general as a range of scales, for which drive and damping are unimportant—occurs mainly due to forward or inverse cascades of conserved quantities, depending on the type of turbulence [12]. This local cascade picture describes primarily the effects of the nonentities.

In the context of plasma physics, it is not clear if such a picture is applicable, even as a qualitative tool for understanding. The free energy source in fusion plasmas usually comes from the gradients of background profiles of density, temperature, etc. This leads to energy injection, via micro-instabilities, at a scale small compared with the size of the device, and not well localized in k -space. Thus, these instabilities can affect the form of the spectrum in a range of scales. Furthermore, for a given set of profiles, it is common to have multiple modes of turbulence driven at various different scales (ion temperature gradient (ITG) driven modes [13], trapped electron modes (TEMs) [14], electron temperature gradient (ETG) driven modes [15], etc) coexisting together. It is difficult in real experimental situations to disentangle these different types of instabilities to see whether there is indeed a local cascade physics somewhere in the background imposed by the structure of the non-linearities.

On the other hand, interactions with large scale modes (e.g. zonal flows) that are linearly stable, may play the role of a ‘sink’ for the drift turbulence acting on a wide range of scales. Kinetic effects such as Landau damping also provide sinks that are not limited to small scales and are naturally anisotropic. These different dynamical effects make any range we observe in plasma turbulence act like a ‘dissipative range’ of neutral fluid turbulence, with a superimposed ‘driving range’ on top of it. In other words, the idea of a cascade may still be useful, but only as an intellectual tool that allows us to reduce the information contained in the full dynamics to conceptual parts that can be understood, and not as a directly observable phenomenon in a wide range of scales as in neutral fluids or astrophysical plasmas.

In this work, we borrow the idea of using shell models to describe the evolution of turbulence spectrum [16] from fluid turbulence and try to develop it to a level where it can be applied to plasma turbulence. Our purpose here is not to write a full description of plasma turbulence using shell models, but to propose a model, simple enough that the effects of each of its basic physical ingredients (such as energy injection or non-linear coupling leading to cascade) can be understood in isolation, but complex enough that it includes at least some of the essential ingredients to be applicable to plasma turbulence. In this paper, for local interactions, we focus on fully developed turbulence due to the fact that it is closer to the standard case studied in neutral fluid turbulence. We leave the question of transition to turbulence and ‘weak turbulence’ regimes (where wave–particle interactions also play an important role) to a future study. We use the weak turbulence form for the disparate scale interactions, which is consistent with the basic idea that weak turbulence is usually dominated by such interactions, i.e. those with zonal flows, convective cells or geodesic acoustic modes (GAMs) [17].

In section 2 we start with the Hasegawa–Mima (H–M) system as the simplest example. We derive a shell model for the H–M system in the absence of linear drive where the assumption of isotropy can be justified. Then, we introduce linear drive and meso-scale structures for this simple system. Then in section 3, we look at the 2 field model of Hasegawa and Wakatani. Again, we first derive the simple shell model and add drive and meso-scales

later on. In section 4 we generalize these findings in the form of a model of isolated potential vorticity (PV) evolution and comment on the resulting steady state spectra. We discuss numerical results corresponding to various implementations of each of these models and their dynamics.

2. Shell model for drift waves

In this section we derive a simple shell model that describes drift wave turbulence. We demonstrate the derivation in this simple case in some detail in order to provide an introduction to the method that is used throughout the paper. The derivations of the shell models in the later sections follow exactly the same logical pattern.

Here, we start by assuming that the turbulence is isotropic and that there is an inertial range ‘far’ from sources and sinks. This should be seen as a first step in building a working shell model. Since these assumptions may not in fact be justified for plasma turbulence, we will later show what they actually correspond to or how to relax them.

2.1. Hasegawa–Mima shell model

As the first step in our formulation, we use the simplest single field model, the H–M model [18], in order to describe the evolution of drift wave turbulence:

$$\partial_t(1 - \nabla^2)\Phi + \partial_y\Phi = \hat{z} \times \nabla\Phi \cdot \nabla\nabla^2\Phi. \quad (1)$$

We use slab geometry, where x corresponds to radial and y to bi-normal ($\hat{z} \times \hat{r}$) directions (sometimes taken simply as the poloidal direction) and z is along the field line. We use a normalization such that the mixing length value is set to 1 (i.e. $\Phi = (e\phi'/T_e/\rho_s/L_n)$, $t = (\rho_s/L_n)\Omega_i t'$ and $\mathbf{x} = \mathbf{x}'/\rho_s$ where primed variables are in physical units). In order to derive a shell model of H–M equation, we take the Fourier transform of (1):

$$\partial_t\Phi_k + \frac{ik_y}{1+k^2}\Phi_k = \frac{1}{2} \sum_{p+q+k=0} \left(\frac{\hat{z} \times \mathbf{p} \cdot \mathbf{q}(p^2 - q^2)}{1+k^2} \right) \Phi_p^* \Phi_q^* \quad (2)$$

and define the shell variable

$$\Phi_n = \left[\frac{1}{(1+k_n^2)} \int_0^{2\pi} d\alpha_k \int_{k_n}^{k_{n+1}} \langle |\tilde{\Phi}_k|^2 (1+k^2) \rangle k dk \right]^{1/2}, \quad (3)$$

where k is the magnitude of the wave-vector and $\langle \cdot \rangle$ denote the average over the fluctuations in a quasi-steady state. The limits in (3) are selected by taking circular ‘shells’ in k -space such that each shell is described by the magnitude of its wave-number $k_n = g^n k_0$ (where $g > 1$ is a measure of logarithmic distance among shells). We use the notation Φ_n consistently throughout the paper to indicate the ‘shell variable’, the variable indicating the total energy in a given shell as in figure 1. The shell variable is defined in the above form because the energy in an infinitesimal shell of thickness dk in two dimensions is given by $E(k) = \int_0^{2\pi} d\alpha_k \langle |\tilde{\Phi}_k|^2 (1+k^2) \rangle k$. Thus, the energy in a shell of finite thickness corresponds to $E_n = \int_{k_n}^{k_{n+1}} E(k) dk$, which we can write as $E_n \equiv |\Phi_n|^2 (1+k_n^2)$.

In fact, the exact form of the shell variable is not very important. However its dimension and the fact that it is integrated over the angular variable $\alpha_k \equiv \text{atan}(k_\theta/k_r)$ are important for a proper interpretation of the result in terms of conserved quantities. For isotropic turbulence, $\langle |\tilde{\Phi}_k|^2 (1+k^2) \rangle$ is independent of α_k and the integration simply gives 2π . The variable Φ_n can

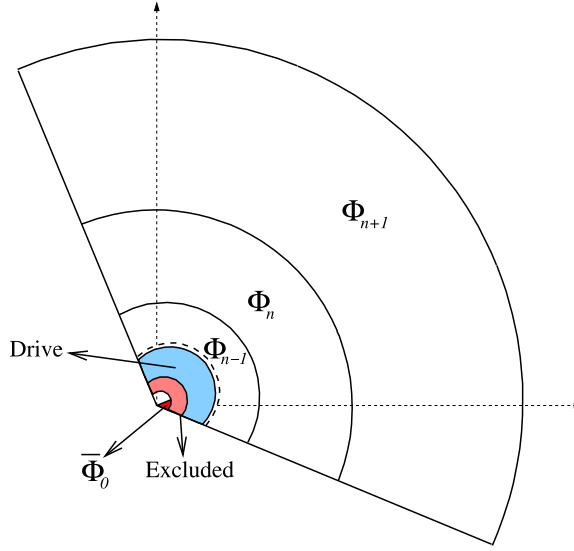


Figure 1. The basic geometry of the shell models.

be defined *even if the turbulence is anisotropic*; however in that case, it only corresponds to the isotropic component (i.e. the ‘monopole’ in a multipole expansion) of turbulence spectra.

We observe from (2) that:

- (i) The interaction coefficient vanishes for $|q| \approx |p|$.
- (ii) The interaction is quadratic.

If we assume the interactions are local in k -space, and that the order of the non-linearity is preserved, we can in general write

$$\partial_t \Phi_n = \sum_{m=-2}^2 \sum_{\ell=-2}^2 A_{nm\ell} \Phi_{n+m} \Phi_{n+\ell}, \quad (4)$$

where $|k_{n+m} \pm k_{n+\ell}| = k_n$ (i.e. the wavenumbers have to match so that a non-linear interaction can take place). Some elements of $A_{nm\ell}$ vanish due to this condition. For instance, if we consider (taking $g = 2$ for simplicity) $k_{n+2} \in [4k, 8k] \pm k_{n-2} \in [k/4, k/2]$, this has no intersection with $k_n \in [k, 2k]$. Thus, a wave-vector from the shell labeled by $n + 2$ and a wavenumber from the shell labeled by $n - 2$, cannot drive non-linearly a wavenumber which falls in the shell labeled by n . This implies therefore that $A_{n,+2,-2}$ has to vanish.

As we noted, if $|q| \approx |p|$, the interaction coefficient vanishes. In contrast if $|p| \approx |k|$ or if $|q| \approx |k|$, the interaction coefficient itself [e.g. $M_{k,p,q} = \hat{z} \times \mathbf{p} \cdot \mathbf{q}(p^2 - q^2)/(1 + k^2)$] does not vanish. However, when we focus on such an interaction (e.g. for simplicity consider the case $\mathbf{p} = k\hat{x}$, $\mathbf{q} = k\hat{x} + k\hat{y}$ and $\mathbf{k} = k\hat{y}$), and consider energy transfer for demonstration, we see that $T_{k,p,q}(E) = -k^4 \Phi_p \Phi_q$, $T_{p,q,k}(E) = k^4 \Phi_q \Phi_k$ whereas $T_{q,k,p}(E) = 0$ (where $T_{k,p,q}(E)$ denotes transfer of energy from \mathbf{p} and \mathbf{q} into \mathbf{k}). In other words, there exists a rather efficient interaction involving wavenumbers of magnitude k and $\sqrt{2}k$, driving a wavenumber with magnitude k . However when integrated over the shell, this interaction does not lead to energy transfer among different shells (i.e. it transfers energy among $\mathbf{p} = k\hat{x}$ and $\mathbf{k} = k\hat{y}$, both of which are in the same shell). Instead, such an interaction simply isotropizes the energy (or enstrophy) within a given shell n . This fact, which can be expressed as ‘interactions involving wavenumbers of same magnitude do not lead to transfer across shells’, gives $A_{n0\ell} = A_{nm0} = 0$.

Similarly, all the diagonal components of $A_{nm\ell}$ (which is rank 2 for given n) must also vanish because of the observation that the interaction coefficient vanishes if $q \approx p$. This leaves us only those coefficients corresponding to the modes which can satisfy the resonance condition, are different from each other and are different from k_n . Hence (4) becomes

$$\partial_t \Phi_n = a_n \Phi_{n-2} \Phi_{n-1} + b_n \Phi_{n-1} \Phi_{n+1} + c_n \Phi_{n+1} \Phi_{n+2}. \quad (5)$$

If we go through each term on the right-hand side, we see that they correspond to interactions

$$k_{n-2} \in [k/4, k/2] + k_{n-1} \in [k/2, k] = k_n \in [k, 2k],$$

$$k_{n+1} \in [2k, 4k] - k_{n-1} \in [k/2, k] = k_n \in [k, 2k]$$

and

$$k_{n+2} \in [4k, 8k] - k_{n+1} \in [2k, 4k] = k_n \in [k, 2k],$$

respectively.

The forms of the truncated interaction coefficients in (5) as functions of shell wavenumber k_n can be determined from the initial form of the interaction coefficient as defined in (2) in terms of interacting wave-vectors. They are

$$a_n = \alpha \frac{k_n^4}{1+k_n^2} \frac{(g^2-1)}{g^7}, \quad b_n = \beta \frac{k_n^4}{1+k_n^2} \frac{(g^4-1)}{g^2} \quad (6)$$

and

$$c_n = \gamma \frac{k_n^4}{1+k_n^2} (g^2-1) g^5. \quad (7)$$

In addition, since the initial system conserves total energy and total potential enstrophy, we argue that the local approximation employed in (5) must also conserve these quantities 2. This will act as a constraint on the coefficients α , β and γ , and by doing so, define the spectrum in the ‘inertial range’.

2.1.1. Energy conservation. Total fluctuation energy as defined by

$$E = \int dk |\tilde{\Phi}_k|^2 (1+k^2)$$

is conserved by the H–M system (i.e. equation (2)). Thus, the same quantity written in terms of the shell variables

$$E = \sum_n \Phi_n^2 (1+k_n^2)$$

has to be conserved by the corresponding shell model (i.e. equation (5)). Multiplying (5) by $(1+k_n^2)\Phi_n$ summing over all n , we obtain the condition

$$\frac{dE}{dt} = \sum_n (1+k_n^2) [a_n \Phi_{n-2} \Phi_{n-1} \Phi_n + b_n \Phi_{n-1} \Phi_{n+1} \Phi_n + c_n \Phi_{n+1} \Phi_{n+2} \Phi_n],$$

which has to vanish. By re-arranging the sum on the right-hand side, we can see that the energy is conserved if

$$a_{n+1}(1+k_{n+1}^2) + b_n(1+k_n^2) + c_{n-1}(1+k_{n-1}^2) = 0.$$

Using $k_{n+1} = gk_n$ and $k_{n-1} = g^{-1}k_n$, we can write this in terms of the coefficients (6) and (7) as

$$\alpha g^{-3} + \beta g^{-2}(g^2+1) + \gamma g = 0. \quad (8)$$

2.1.2. Enstrophy conservation. For the pure H–M system, another conserved quantity is enstrophy, which is defined as

$$W = \int d\mathbf{k} |\tilde{\Phi}_k|^2 k^2 (1 + k^2) = \sum_n \Phi_n^2 (1 + k_n^2) k_n^2.$$

Multiplying (5) by $(1 + k_n^2) k_n^2 \Phi_n$, summing over all n and re-arranging the resulting sum, we find that the total fluctuation potential enstrophy is conserved if

$$a_{n+1} (1 + k_{n+1}^2) k_{n+1}^2 + b_n (1 + k_n^2) k_n^2 + c_{n-1} (1 + k_{n-1}^2) k_{n-1}^2 = 0$$

and in terms of coefficient α , β and γ , this gives

$$\alpha g^{-1} + \beta g^{-2} (g^2 + 1) + \gamma g^{-1} = 0. \quad (9)$$

Taken together with equation (8), this implies

$$\beta = -\alpha g^{-1} \quad \text{and} \quad \gamma = \alpha g^{-2}.$$

This condition, on these otherwise arbitrary coefficients, gives us a severely truncated system where the scales (represented by shells) non-linearly interact among themselves locally and in the same way as the original H–M system does, and preserve energy and enstrophy while doing so.

2.1.3. The model and the steady state spectra. The simple shell model for the pure H–M system, conserving energy and enstrophy can be written as

$$\frac{\partial \Phi_n}{\partial t} = \alpha \frac{k_n^4 (g^2 - 1)}{1 + k_n^2} [g^{-7} \Phi_{n-2} \Phi_{n-1} - (g^2 + 1) g^{-3} \Phi_{n-1} \Phi_{n+1} + g^3 \Phi_{n+1} \Phi_{n+2}]. \quad (10)$$

This describes only the local interactions in some hypothetical ‘inertial range’. This is effectively the model, introduced in [19]. There is neither any drive nor any damping in this system. It is obviously overly simple. However, it allows us to isolate the effect of local interactions in a drift wave type nonlinearity. Taking the steady state limit, assuming a power law form (i.e. $\Phi_n \propto k_n^\lambda$), substituting into (10) and noting $k_{n+m}^\lambda = g^{m\lambda} k_n^\lambda$, we find

$$[g^{-7} g^{-3\lambda} - (g^2 + 1) g^{-3} + g^{3+3\lambda}] = 0.$$

It is easy to see that this can be satisfied by $\lambda = -4/3$ or $\lambda = -2$. This means we have the two possible steady state solutions

$$\Phi_n \propto k_n^{-2} \quad \text{and} \quad \Phi_n \propto k_n^{-4/3}$$

for this system. These actually correspond to the well-known Kraichnan–Kolmogorov dual cascade solutions, which, when written in terms of $|\Phi(k)|^2$ are

$$|\Phi_k|^2 \propto k^{-6} \quad \text{and} \quad |\Phi_k|^2 \propto k^{-14/3}.$$

If one computes the energy density $E(k)$ as defined for the Euler system using the above forms for $|\Phi_k|^2$'s (i.e. $E(k) \approx k^3 |\Phi_k|^2$) one would in fact obtain the more familiar forms with powers $-5/3$ and -3 . However, for the H–M system the definition of the energy density also involves a $(1 + k^2)$ and therefore it does not give a perfect power law. Because of this, we will consistently use fluctuation spectra as given above in this paper, and not the energy density spectra.

2.1.4. Realizability and phase dynamics. The shell variable Φ_n as defined in (3) does not have a well-defined phase. In other words, one can take Φ_n to be either the positive or the

negative root of the square root in (3), and the value of energy would not change. As a result its evolution given by equation (10) does not guarantee positive definiteness. Let us take $\Phi_n > 0$ for all n with an initial distribution such that $\Phi_n \sim \Phi_{n-2} \sim \Phi_{n+2} \sim 0$ and $\Phi_{n+1} \sim \Phi_{n-1} \gg 0$. In this case, $\partial \Phi_n / \partial t$ will be negative, and since $\Phi_n \sim 0$, Φ_n will become negative in the next time step.

Because of this, it is common to generalize Φ_n to include complex phase, and allow the model equations to evolve phase as well as amplitude. For instance, one can introduce

$$\frac{\partial \Phi_n}{\partial t} = \alpha \frac{k_n^4 (g^2 - 1)}{1 + k_n^2} [g^{-7} \Phi_{n-2} \Phi_{n-1} - (g^2 + 1) g^{-3} \Phi_{n-1}^* \Phi_{n+1} + g^3 \Phi_{n+1}^* \Phi_{n+2}]. \quad (11)$$

Here the complex conjugates are selected such that if the contributing k is negative (e.g. $n + 1$ in $k_n = k_{n+2} - k_{n+1}$) its shell variable is conjugated, since for instance $\Phi_{n+1}^* \sim (A_{n+1} e^{ik_{n+1}x})^* \sim A_{n+1} e^{-ik_{n+1}x}$, whereas if the contributing k is positive (e.g. $n - 1$ or $n - 2$ in $k_n = k_{n-1} + k_{n-2}$), it is not. In contrast, the Glezder–Ohkitani–Yamada (GOY) model [20] has all the terms on the right-hand side conjugated. Note that other alternatives exist in the literature [21]. The generalization of the shell variable as a complex variable and the introduction of phase evolution allow shell models to be implemented numerically more easily, since for small values of Φ_n , a change in the sign simply leads to a change in the phase dynamics and this does not change the conserved quantities.

Also, equation (11) remains invariant under a transformation of the form $\Phi_n = \Phi_n e^{i\theta_n}$, if $\theta_{n+1} - \theta_{n-1} - \theta_n = 0$. This suggests that it has the same properties, in terms of phase dynamics, as the model of [21]. Note that for the steady state analytical solutions, realizability is not an issue. In that case, one can safely disregard the phase dynamics and consider Φ_n as a positive definite quantity.

2.1.5. The continuum limit. We find it surprising that the continuum limits of shell models are not widely studied, even in fluid dynamics. Going through the literature one finds that the main reference used in neutral fluids literature for the continuum limit of the GOY model is ‘unpublished’ [22, 23]. Therefore, we decided to provide a detailed derivation of the continuum limit of the above shell model in appendix A, which we will use as a basic reference when we deal with more complicated shell models. The result in compact notation is

$$\frac{\partial \Phi(k)}{\partial t} = \frac{3\alpha\epsilon^{7/2}}{(1+k^2)\Phi(k)} \frac{1}{k} \frac{\partial}{\partial k} \left(k^2 \Phi(k) \frac{\partial}{\partial k} [k^6 \Phi(k)^2] \right), \quad (12)$$

where $\Phi(k_n) \equiv \Phi_n / \sqrt{2\pi k_n \Delta k_n}$ as Δk_n goes to zero. Here α is the coefficient of interaction which denotes the strength of the non-linearity and ϵ is the small parameter of the shell spacing (i.e. $g = 1 + \epsilon$, see appendix A for details). This is the continuum limit of the shell model for the Hasegawa–Mima system. If we take the Euler limit [i.e. $(1+k^2) \rightarrow k^2$] and use the energy within an infinitesimal shell for the Euler system [i.e. $E(k) = k^3 \Phi(k)^2$], we get

$$\frac{\partial E}{\partial t} = \frac{\partial}{\partial k} \left(D \sqrt{kE} \frac{\partial}{\partial k} [k^3 E] \right),$$

where $D = 3\alpha\epsilon^{7/2}$. This is nothing but the first order ‘differential approximation model’ (DAM) for the Euler system [24, 25]. It would be interesting to continue the expansion and see if the agreement persists in higher orders.

2.2. Disparate scale interactions

While the possibility of excitation of large scale flow structures from small scale plasma turbulence via parametric and modulational instabilities has been known for a long time [26],

the key role these flow structures play in plasma transport has been recognized in the last few decades [17]. Here by large scale flows, we usually denote zonal flows; however, in general they correspond to $k_{\parallel} = 0$ modes, which may be zonal flows, GAMs or non-linear streamers. Since these structures play an important role in transport, their effect on wavenumber and frequency spectrum of micro-turbulence is also expected to be important. Including the effect of large scale flows in the shell model picture is non-trivial. First, one must choose the correct invariants that the full system consisting of fluctuations and the large scale flows conserve.

In order to do that, we suggest the following simple, self-consistent system of equations, on which we base our shell model derivation [27, 28]:

$$\begin{aligned} (\partial_t + \hat{z} \times \nabla \bar{\Phi} \cdot \nabla)(\tilde{\Phi} - \nabla^2 \tilde{\Phi}) + \hat{z} \times \nabla \tilde{\Phi} \cdot \nabla(n_0(x) - \nabla^2 \bar{\Phi}) \\ = (\hat{z} \times \nabla \tilde{\Phi} \cdot \nabla \nabla^2 \tilde{\Phi} - \langle \hat{z} \times \nabla \tilde{\Phi} \cdot \nabla \nabla^2 \tilde{\Phi} \rangle), \end{aligned} \quad (13)$$

$$\partial_t(n_0(x) - \nabla^2 \bar{\Phi}) = \langle \hat{z} \times \nabla \tilde{\Phi} \cdot \nabla \nabla^2 \tilde{\Phi} \rangle, \quad (14)$$

where as usual \hat{z} is along the direction of the background magnetic field. These two equations correspond simply to the advection of PV in two dimensions [29, 30], defined for drift waves as

$$h \equiv \bar{h} + \tilde{h} = (n_0(x) + \tilde{\Phi}) - (\nabla^2 \tilde{\Phi} + \nabla^2 \bar{\Phi}).$$

Here $n(x)$ is a fixed background density profile, $\langle \cdot \rangle$ denote an average over fluctuations, $\bar{\Phi}$ is the mean component (i.e. slowly evolving in time, $k_{\parallel} = 0$, etc) of the electrostatic potential corresponding to the large scale flow (i.e. $\bar{v} \equiv \hat{z} \times \nabla \bar{\Phi}$) and $\tilde{\Phi}$ is the fluctuating electrostatic field corresponding to micro-turbulence. Note that $\bar{\Phi}$ does not appear in PV explicitly due to the way electrons respond to fluctuations versus the mean flow. This is an important point which affects the non-linear structure of the equations. The right-hand side of (13) describes mode-coupling between fluctuations while the terms on the left describe interactions with the mean flow. Note also that the fluctuation equation reduces to the H-M equation when $\bar{\Phi} = \partial_t \bar{\Phi} = 0$.

The disparate scale interactions as described by (13) and (14) conserve potential enstrophy:

$$Z \equiv \langle (\nabla^2 \bar{\Phi})^2 + (\tilde{\Phi} - \nabla^2 \tilde{\Phi})^2 \rangle$$

while local interactions among fluctuations are still described by the conservation laws (and thus by the shell model) derived earlier. In order to add an equation for the mean flow (i.e. $k_{\parallel} \approx 0$ mode) we note that in the shell model picture, the mean flow interacts with every single shell directly (i.e. non-locally) and exchanges potential enstrophy with each shell by refracting its wavenumber to larger k (i.e. toward shells with larger n). Using (13) and (14), we can write the truncated equations as

$$\frac{\partial}{\partial t} \bar{\Phi} + \sum_n a_n \Phi_n \Phi_{n+1} + \nu_F \bar{\Phi} = 0 \quad (15)$$

and

$$\frac{\partial \Phi_n}{\partial t} + b_n \bar{\Phi} \Phi_{n+1} + c_n \bar{\Phi} \Phi_{n-1} = C(\Phi_n, \Phi_n), \quad (16)$$

where a_n , b_n and c_n are

$$a_n = -\bar{\alpha} \frac{k_n^3 g (g^2 - 1)}{q}, \quad b_n \approx \bar{\alpha} \frac{q k_n g (1 + g^2 k_n^2 - q^2)}{1 + k_n^2}$$

and

$$c_n \approx -g \bar{\alpha} \frac{q k_n g^{-1} (1 + g^{-2} k_n^2 - q^2)}{1 + k_n^2}.$$

The forms of these coefficients are determined exactly the same way as in the previous section; however, this time using conservation of total potential enstrophy Z . In (16), $C(\Phi, \Phi)$ represents local interactions among shells in the absence of mean flows. We take this from equation (10) since we expect the local interactions to conserve total fluctuation enstrophy as before

$$C(\Phi_n, \Phi_n) \equiv \alpha \frac{k_n^4 (g^2 - 1)}{1 + k_n^2} [g^{-7} \Phi_{n-2} \Phi_{n-1} - (g^2 + 1) g^{-3} \Phi_{n-1} \Phi_{n+1} + g^3 \Phi_{n+1} \Phi_{n+2}].$$

The resulting shell model can be written as

$$\frac{\partial \Phi_n}{\partial t} + \bar{\alpha} \frac{q k_n \bar{\Phi}}{1 + k_n^2} [g(1 + g^2 k_n^2 - q^2) \Phi_{n+1} - (1 + g^{-2} k_n^2 - q^2) \Phi_{n-1}] = C(\Phi_n, \Phi_n), \quad (17)$$

$$\frac{\partial}{\partial t} (q^2 \bar{\Phi}) = \bar{\alpha} \sum_n q k_n^3 g (g^2 - 1) \Phi_n \Phi_{n+1} - \nu_F q^2 \bar{\Phi}. \quad (18)$$

This is a coupled system, describing the evolution of drift wave turbulence undergoing local cascade and interacting with a large scale mode which evolves self-consistently with drift wave turbulence.

2.2.1. Stationary spectrum with disparate scale interactions. We can obtain the steady state fluctuation spectrum when disparate scale interactions dominate using (17) and considering only the second term on the left-hand side. This gives

$$[g(1 - q^2 + g^2 k_n^2) \Phi_{n+1} - (1 - q^2 + g^{-2} k_n^2) \Phi_{n-1}] = 0$$

which has the solution

$$\Phi_n \sim \frac{k_n^{-1/2}}{(1 - q^2 + k_n^2)},$$

or when written in terms of the fluctuation intensity, this implies (for $q \ll k$)

$$|\tilde{\Phi}_k|^2 \sim \frac{k^{-3}}{(1 - q^2 + k^2)^2} \sim \frac{k^{-3}}{(1 + k^2)^2}. \quad (19)$$

This is the steady state spectrum when there is a large scale mode and the disparate scale interactions with this mode are dominant. Note that large scale here is effectively defined as a $k_{\parallel} \approx 0$ with a $|k|$ smaller compared with the range for which we observe the turbulence. Generally these are zonal flows. However, other meso-scale modes or external mean flows may become dominant if zonal flows are weak or artificially suppressed.

2.2.2. Continuum limit. Repeating the continuum limit calculation of section 2.1.5 (given in appendix A), for the model given in (17) and (18):

$$\epsilon^{1/2} k \frac{\partial \Phi(k)}{\partial t} + \bar{\alpha} \epsilon^{1/2} \frac{q k^2 \bar{\Phi}}{(1 + k^2)} \left[2(1 - q^2 + k^2) k \Phi'(k) + 3 \left(1 - q^2 + \frac{7}{3} k^2 \right) \Phi(k) \right] = C(\Phi, \Phi)$$

which we can re-write in the form

$$\begin{aligned} \frac{\partial \Phi(k)}{\partial t} + \frac{2\bar{\alpha}\epsilon k^{1/2}}{(1 + k^2)} \frac{\partial}{\partial k} (q \bar{\Phi} k^{3/2} [1 - q^2 + k^2] \Phi(k)) \\ = \frac{3\alpha\epsilon^{7/2}}{(1 + k^2)\Phi(k)} \frac{1}{k} \frac{\partial}{\partial k} \left(k^2 \Phi(k) \frac{\partial}{\partial k} [k^6 \Phi(k)^2] \right) \end{aligned} \quad (20)$$

and for the mean flows

$$\left(\frac{\partial}{\partial t} + v_F\right)(q^2\bar{\Phi}) = 2\bar{\alpha}q \int_{k_{\min}}^{\infty} [k^4\Phi(k)^2] dk.$$

The form of (20) is interesting, in particular in the limit $q \ll k$, if we write the equation for fluctuation potential enstrophy:

$$\begin{aligned} \frac{\partial}{\partial t} [(1+k^2)^2\Phi(k)^2] + \bar{\alpha}\epsilon \frac{1}{k} \frac{\partial}{\partial k} (k[k^2q\bar{\Phi}(1+k^2)^2\Phi(k)^2]) \\ = 3\alpha\epsilon^{7/2}(1+k^2) \frac{1}{k} \frac{\partial}{\partial k} \left(k^2\Phi(k) \frac{\partial}{\partial k} [k^6\Phi(k)^2] \right), \end{aligned}$$

or

$$\frac{\partial}{\partial t} N_k + \bar{\alpha}\epsilon \nabla_k \cdot [k^2q\bar{\Phi}N_k] = C'(N_k, N_k) \quad (21)$$

if we let $N_k \equiv [(1+k^2)^2\Phi(k)^2]$. This equation is remarkably similar to the wave-kinetic equation:

$$\begin{aligned} \frac{\partial}{\partial t} N_k(\mathbf{X}, t) + \nabla_k \cdot [(\omega - \bar{\mathbf{V}} \cdot \mathbf{k}) \nabla_{\mathbf{X}} N_k(\mathbf{X}, t)] \\ - \nabla_{\mathbf{X}} \cdot [(\omega - \bar{\mathbf{V}} \cdot \mathbf{k}) \nabla_k N_k(\mathbf{X}, t)] = C'(N_k, N_k). \end{aligned} \quad (22)$$

In order to obtain (21) starting from (22), we would need to define

$$N_k \equiv \int d\alpha_k \int N_k(\mathbf{X}, t) d\mathbf{X}$$

which is integrated over the k -space angular variable $\alpha_k \equiv \text{atan}(k_\theta/k_r)$ as well as the slow spatial variable. Since there is no other spatial scale associated with the fluctuation spectrum, we assert that

$$\int d\alpha_k \int \nabla_{\mathbf{X}} N_k(\mathbf{X}, t) d\mathbf{X} = \alpha' \epsilon k N_k$$

which is consistent with an assumption of scale separation (but implies a particular scaling of the spatial gradient of intensity). Here α' is an unknown constant. If we further assume that small scale evolution remains sufficiently isotropic, we can indeed recover (21).

2.3. Comparison with Tore-Supra measurements

The turbulence spectrum in tokamaks can be measured using different methods. Here, we demonstrate a standard, Ohmic, L-mode shot from Tore-Supra tokamak measured using the Doppler reflectometer system, DifDop (figure 2). The figure shows a reasonably good agreement between the measured spectrum and the analytical expression $k^{-3}/(1+k^2)^2$. Of course, one can find better fits, with different functional forms. For instance, as one goes to higher k , the spectrum will ultimately take the form of an exponential, which suggests that we observe a ‘dissipation’ range. For instance in the case of disparate scale interactions and a physical mechanism of damping that goes as $\gamma_d(k) \sim -\lambda_d k^2$, one does indeed recover a scaling: [31]

$$\langle |\tilde{n}_k|^2 \rangle \sim \langle |\tilde{\Phi}_k|^2 \rangle \sim \frac{k^{-3}}{(1+k^2)^2} e^{-\lambda k}.$$

Or one can simply use an exponential function directly. However, the expression $k^{-3}/(1+k^2)$ does not have any fitting parameters (apart from the fluctuation level), and can be linked to the physical process of disparate scale interactions. Therefore its agreement with experiment is remarkable and arguably more informative than a fit with an exponential function, which has a fitting parameter and implies a dissipative scaling.

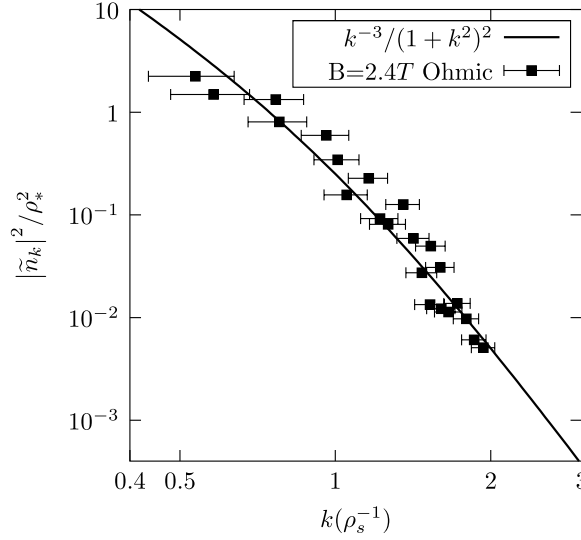


Figure 2. Measurement of density fluctuation spectrum in a standard Ohmic discharge in Tore Supra tokamak. The analytical formula seems to agree reasonably well with the observations. Note that the error bars in the figure indicate the error only in the measurement of k . Here an average value of ρ_s is used for normalization. An error in this would simply shift all the measured points to the left or to the right. Note also that since there is no absolute calibration of the experimental setup for the fluctuation level, the y-axis is effectively in arbitrary units.

3. Shell model for Hasegawa–Wakatani (H–W) system

3.1. The model

The H–W system consists of the equations

$$\frac{\partial n}{\partial t} + v_n \frac{\partial \Phi}{\partial y} - \eta k_{\parallel}^2 (\Phi - n) - D_n \nabla^2 n = -\hat{z} \times \nabla \Phi \cdot \nabla n, \quad (23)$$

$$\frac{\partial \nabla^2 \Phi}{\partial t} - \eta k_{\parallel}^2 (\Phi - n) - \nu \nabla^2 \nabla^2 \Phi + \mu \nabla^2 \Phi = -\hat{z} \times \nabla \Phi \cdot \nabla \nabla^2 \Phi. \quad (24)$$

ITG or another similar model has the same basic non-linear structure, while the linear dynamics can be very different. Here we focus on fully developed turbulence and the effects of non-linear terms.

It is well known that the non-linear terms in the H–W system conserve kinetic energy

$$E = \sum_k |\Phi_k|^2 k^2,$$

internal energy

$$N = \sum_k |n_k|^2,$$

enstrophy

$$W = \sum_k |\Phi_k|^2 k^4,$$

and the cross correlation which can be called ‘effective helicity’

$$H = \sum_k \text{Re}[k^2 \Phi_k n_k].$$

As in the previous sections, we want to derive a shell model, where the non-linear interactions can be modeled by local couplings but still conserve these primary quantities. The shell variables are defined as

$$\Phi_n \equiv \left[\frac{2\pi}{k_n^2} \int_{k_n}^{k_{n+1}} |\Phi_k|^2 k^3 dk \right]^{1/2}, \quad (25)$$

$$n_n \equiv \left[2\pi \int_{k_n}^{k_{n+1}} |n_k|^2 k dk \right]^{1/2}. \quad (26)$$

The standard truncation corresponding to keeping only local interactions has the form

$$\begin{aligned} \frac{\partial n_n}{\partial t} + \mathcal{L}_n(\Phi_n, n_n) = & a_n(\Phi_{n-2}n_{n-1} - \Phi_{n-1}n_{n-2}) + b_n(\Phi_{n-1}n_{n+1} - \Phi_{n+1}n_{n-1}) \\ & + c_n(\Phi_{n+1}n_{n+2} - \Phi_{n+2}n_{n+1}), \end{aligned} \quad (27)$$

$$\frac{\partial \Phi_n}{\partial t} + \mathcal{L}_\phi(\Phi_n, n_n) = a'_n(\Phi_{n-2}\Phi_{n-1}) + b'_n(\Phi_{n-1}\Phi_{n+1}) + c'_n(\Phi_{n+1}\Phi_{n+2}). \quad (28)$$

Comparing with the Fourier transforms of (23) and (24), we see that

$$a_n \approx \alpha k_{n-2}k_{n-1} = \alpha k_n^2 g^{-3}, \quad (29)$$

$$b_n \approx \beta k_n^2, \quad c_n \approx \gamma k_n^2 g^3 \quad (30)$$

and

$$a'_n \approx \alpha' \frac{k_{n-1}k_{n-2}(k_{n-1}^2 - k_{n-2}^2)}{k_n^2} = \alpha' k_n^2 (g^2 - 1)g^{-7}, \quad (31)$$

$$b'_n \approx \beta' k_n^2 (g^4 - 1)g^{-2}, \quad c'_n = \gamma' k_n^2 (g^2 - 1)g^5. \quad (32)$$

As usual, we use the conservation laws in order to derive relationships among these coefficients, which leads to the shell model for the H–W system:

$$\begin{aligned} \frac{\partial n_n}{\partial t} + \mathcal{L}_n(\Phi_n, n_n) = & \alpha k_n^2 [g^{-3}(\Phi_{n-2}n_{n-1} - \Phi_{n-1}n_{n-2}) - g^{-1}(\Phi_{n-1}n_{n+1} - \Phi_{n+1}n_{n-1}) \\ & + g(\Phi_{n+1}n_{n+2} - \Phi_{n+2}n_{n+1})], \end{aligned} \quad (33)$$

$$\begin{aligned} \frac{\partial \Phi_n}{\partial t} + \mathcal{L}_\phi(\Phi_n, n_n) = & \alpha k_n^2 (g^2 - 1) [g^{-7}\Phi_{n-2}\Phi_{n-1} - (g^2 + 1)g^{-3}\Phi_{n-1}\Phi_{n+1} \\ & + g^3(\Phi_{n+1}\Phi_{n+2})]. \end{aligned} \quad (34)$$

We argue that the linear dynamics are important mainly for energy injection and do not play a key role in the inertial range. Thus neglecting the linear terms and substituting $\Phi_n \propto k_n^\lambda$ into (34), we get $\lambda = -4/3$ or $\lambda = -2$ as in the case of pure H–M turbulence. These correspond to the standard dual cascade spectra in 2D turbulence.

3.2. Stationary spectra of density fluctuations

We already know that the stationary spectra for Φ in the inertial range is either $\Phi_n \propto k_n^{-4/3}$ or $\Phi_n \propto k_n^{-2}$. We consider these two cases separately, assuming $n_n \propto k_n^\chi$.

3.2.1. $\Phi_n \propto k_n^{-4/3}$ case. If we ignore linear dynamics and substitute $\Phi_n \propto k_n^{-4/3}$ and $n_n \propto k_n^\chi$ into (33), we obtain

$$(g^{-\chi-1/3} - g^{-5/3} g^{-2\chi}) - (g^{1/3+\chi} - g^{-7/3-\chi}) + (g^{2\chi-1/3} - g^{\chi-5/3}) = 0 \quad (35)$$

since g is by definition positive and greater than one, the only way this vanishes is if a term with a plus sign cancels a term with a minus sign. Considering each permutation, we find that the possible values of χ that satisfy (35) are $\chi = -4/3$, $\chi = -1/3$ and $\chi = 2/3$. For $|n_k|^2$ these imply

$$\begin{aligned} n_n \propto k_n^{-4/3} &\rightarrow |n_k|^2 \propto k^{-14/3}, \\ n_n \propto k_n^{-1/3} &\rightarrow |n_k|^2 \propto k^{-8/3}, \\ n_n \propto k_n^{2/3} &\rightarrow |n_k|^2 \propto k^{-2/3}. \end{aligned}$$

It is interesting to note that, while the $-14/3$ case displays the same scaling with $|\Phi_k|^2 \propto k^{-14/3}$ and thus is possible also in the near-adiabatic limit of the H–W system, the case $-8/3$ corresponds to the fluid limit and is in fact Kraichnan's $k^{-5/3}$ spectrum, but written for internal energy density [i.e. $F(k) = k|n_k|^2 \propto k^{-5/3}$].

3.2.2. $\Phi_n \propto k_n^{-2}$ case. If, on the other hand, we substitute $\Phi_n \propto k_n^{-2}$ and $n_n \propto k_n^\chi$ into (33), we obtain $\chi = -2$, $\chi = 0$ or $\chi = 2$. The scalings for $|n_k|^2$ implied by this are

$$\begin{aligned} n_n \propto k_n^{-2} &\Rightarrow |n_k|^2 \propto k^{-6}, \\ n_n \propto k_n^0 &\Rightarrow |n_k|^2 \propto k^{-2}, \\ n_n \propto k_n^2 &\Rightarrow |n_k|^2 \propto k^2. \end{aligned}$$

Note that while the first one corresponds to the forward energy cascade result of 2D turbulence with adiabatic electrons, the latter is Batchelor's passive scalar spectrum [i.e. $F(k) \propto k^{-1}$]. It is also interesting to note that the difference between these two power laws is 4, which seems to be a generic feature of both experimental results and of theory based on PV evolution.

3.3. Adding drive and disparate scale interactions

The simplest way to introduce linear drive into this model is to add a $\gamma_n \Phi_n$ into (34) and a $\gamma_n n_n$ into (33). Note that, since the shell variable does not contain any phase information, this is not as bad an approximation as it initially seems. However, when we add drive in the presence of an inverse cascade, we also need to consider the large scale structures and their evolution. In fact, the question of saturation depends strongly on the saturation mechanism for these large scale modes.

It is the total energy, enstrophy, etc of the convective cell + the drift waves that should be conserved. It can be verified that the disparate scale interactions in the truncation given by

$$\frac{\partial n_n}{\partial t} = \gamma_n n_n + \bar{\alpha} q k_n [g^{-1}(\bar{\Phi} n_{n-1} - \bar{n} \Phi_{n-1}) - (\bar{\Phi} n_{n+1} - \bar{n} \Phi_{n+1})] + C(\Phi, n), \quad (36)$$

$$\frac{\partial \Phi_n}{\partial t} = \gamma_n \Phi_n + \bar{\alpha} q k_n^{-1} (k_n^2 g^{-2} - q^2) [g^{-1} \bar{\Phi} \Phi_{n-1} - \bar{\Phi} \Phi_{n+1}] + C(\Phi, \Phi), \quad (37)$$

$$\frac{\partial \bar{n}}{\partial t} = \sum_n \bar{\alpha} q k_n (\Phi_n n_{n+1} - \Phi_{n+1} n_n), \quad (38)$$

$$\frac{\partial \bar{\Phi}}{\partial t} = \sum_n \bar{\alpha} (g^2 - 1) q k_n^3 g^{-2} \Phi_n \Phi_{n+1} - v_{ZF} \bar{\Phi} \quad (39)$$

indeed conserve total internal energy $N = \bar{n}^2 + \sum_n n_n^2$, total kinetic energy $K = q^2 \bar{\Phi}^2 + \sum_n k_n^2 \Phi_n^2$, total enstrophy $W = q^4 \bar{\Phi}^2 + \sum_n k_n^4 \Phi_n^4$, total effective helicity $H = q^2 \bar{\Phi} \bar{n} + \sum_n k_n^2 n_n \Phi_n$ and incidentally, also the total potential enstrophy $Z = N + 2H + W$. Here $C(\Phi, n)$ and $C(\Phi, \Phi)$ describe local interactions which conserve the fluctuating energy, enstrophy, etc and therefore are taken from (33) and (34) as

$$C(\Phi, n) \equiv \alpha k_n^2 \{g^{-3}(\Phi_{n-2} n_{n-1} - \Phi_{n-1} n_{n-2}) - g^{-1}(\Phi_{n-1} n_{n+1} - \Phi_{n+1} n_{n-1}) + g(\Phi_{n+1} n_{n+2} - \Phi_{n+2} n_{n+1})\}, \quad (40)$$

$$C(\Phi, \Phi) = \alpha k_n^2 (g^2 - 1) \{g^{-7}(\Phi_{n-2} \Phi_{n-1}) - (g^2 + 1)g^{-3}(\Phi_{n-1} \Phi_{n+1}) + g^3(\Phi_{n+1} \Phi_{n+2})\}. \quad (41)$$

4. Generalization in terms of PV

The results of sections 2.2 and 3.3 suggest that PV dynamics play a crucial role in the evolution of fluctuation spectra. It is possible to generalize these results in terms of PV. We can form

$$h_n = n_n + k_n^2 \Phi_n$$

by multiplying (37) with k_n^2 and summing it with (36). The result is

$$\frac{\partial h_n}{\partial t} = \gamma_n h_n - \bar{\alpha} q k_n [(\bar{\Phi} h_{n+1} - \bar{h} \Phi_{n+1}) - g^{-1}(\bar{\Phi} h_{n-1} - \bar{h} \Phi_{n-1})] + C(\Phi, h), \quad (42)$$

where $\bar{h} = \bar{n} + q^2 \bar{\Phi}$. Note that here $h_{n+1} = n_{n+1} + g^2 k_n^2 \Phi_{n+1}^2$, etc. For the local interaction terms, we have $C(\Phi, h) = C(\Phi, n) + k_n^2 C(\Phi, \Phi)$, using (40) and (41) we indeed obtain

$$C(\Phi, h) \equiv \alpha k_n^2 \{g^{-3}(\Phi_{n-2} h_{n-1} - \Phi_{n-1} h_{n-2}) - g^{-1}(\Phi_{n-1} h_{n+1} - \Phi_{n+1} h_{n-1}) + g(\Phi_{n+1} h_{n+2} - \Phi_{n+2} h_{n+1})\}, \quad (43)$$

which is exactly the same as (40), with n replaced by h . This is not really surprising since the H–W system can be described as advection of PV, and if we only consider the non-linear interaction term the n equation is an equation for a passive scalar. Naturally these two yield rather similar non-linear behavior. Similarly for the large scales, the PV is defined as

$$\bar{h} = \bar{n} + q^2 \bar{\Phi}$$

whose evolution can be computed using (38) and (39) as

$$\frac{\partial \bar{h}}{\partial t} = \bar{\alpha} \sum_n q k_n (\Phi_n h_{n+1} - \Phi_{n+1} h_n) - v_{ZF} \bar{h}. \quad (44)$$

Similarly the H–M with disparate scale interactions (e.g. equations (15) and (16)) can be written in the above form if we define

$$h_n = (1 + k_n^2) \Phi_n.$$

Obviously, this is no coincidence. The system consisting of (42) and (44) can in fact be derived from the general principle of PV conservation. Both the H–M and the H–W systems described above, and more complex systems such as ITG or ETG modes (up to curvature effects), can in fact be recast into a form of advection of PV, except that the PV for each system is different. For instance, a simple slab-ITG model can be formulated as advection of $h = n - \nabla^2 \Phi - P/\Gamma$ (where P is pressure and Γ is the adiabaticity coefficient) [32] when curvature effects are neglected.

If we start from

$$\frac{dh}{dt} = 0$$

and separate it into fluctuation, mean and background parts as

$$h = h_0(x) + \bar{h}(\mathbf{x}, t) + \tilde{h}(\mathbf{x}, t)$$

we obtain

$$\frac{\partial \tilde{h}}{\partial t} + \hat{z} \times \nabla \bar{\Phi} \cdot \nabla \tilde{h} + \hat{z} \times \nabla \tilde{\Phi} \cdot \nabla \bar{h} - \partial_y \tilde{\Phi} \frac{d}{dx} h_0(x) = \hat{z} \times \nabla \tilde{\Phi} \cdot \nabla \tilde{h} - \langle \hat{z} \times \nabla \tilde{\Phi} \cdot \nabla \tilde{h} \rangle$$

and

$$\frac{\partial \bar{h}}{\partial t} = \langle \hat{z} \times \nabla \tilde{\Phi} \cdot \nabla \tilde{h} \rangle,$$

using the usual truncation procedure, and imposing conservation of potential enstrophy

$$Z = \bar{h}^2 + \sum_n h_n^2$$

we can, in fact, derive the system of equations given in (42)–(44).

Of course, in order to actually use this system, one needs an equation for the evolution of Φ , the active field, in most cases. One notable exception is the case when the interactions with the large scale mean flows dominate over everything else. In this case, the steady state spectrum can be computed by the balance

$$\bar{\Phi}[h_{n+1} - g^{-1}h_{n-1}] = 0$$

whose solution is $h_n \propto k_n^{-1/2}$, and this gives for the PV spectrum that

$$|\tilde{h}_k|^2 \propto k^{-3}$$

or in the limit of H–M, this gives

$$|\tilde{\Phi}_k|^2 \sim |\tilde{h}_k|^2 \propto \frac{k^{-3}}{(1+k^2)^2}. \quad (45)$$

5. Numerical studies

The shell models are very useful tools suitable for numerical integration. They can be implemented with a very low number of degrees of freedom and yet they can be used to describe a wide range of scales, and be integrated for a relatively long time. However, since they include a wide range of k_n and Φ_n values, they are also intrinsically stiff. This makes their numerical implementation non-trivial. Furthermore, since the shell models involve terms that are similar to ‘finite-difference’ representations of partial derivatives, the usual problems related to numerical stability of finite-difference schemes also plague them. What is worse is, since the shell model description does not really involve finite-difference representations of continuous operators, one cannot simply replace a term that looks like a finite-difference Euler formula with a higher order finite-difference formula. Nonetheless, we consider shell models as valuable tools once these technicalities are attended to.

We used various methods (including implicit Crank–Nicolson scheme with operator splitting and adaptive time step) for numerical implementation using Gnu Scientific Library (GSL) [33]. In all the cases considered, it is the zonal flow interaction term, i.e. the term

$$\frac{\partial h_n}{\partial t} = -\alpha' q k_n \bar{\Phi}[g h_{n+1} - h_{n-1}] \quad (46)$$

that limits numerical stability properties. This is also the dominant term that defines the shape of the steady state or oscillating spectrum. Using the similarity of this term to a central difference

Euler representation of an advection operator we make sure that Δt_{adv} remains always small compared with $(g - 1)/\alpha'q\bar{\Phi}$, in order to guarantee stability.

In the case when the disparate scale interactions dominate, the term given in (46) leads to negative amplitudes (consistently reversed phases) if a positive derivative in some region is maintained by the drive. Consider for instance that $\Phi_3 > \Phi_1$, and Φ_3 is driven so that this configuration is maintained, in this case Φ_2 will consistently experience a pull toward the negative direction. In order to avoid this, we omit the region corresponding to the scales between the driving scale and the large scale. This means that the local inverse cascade is excluded when the interaction with the large scale is included. Note that this is consistent with the physical assumption of scale separation inherent in the disparate scale interaction picture. We use open boundary conditions on the left ($\Phi_1 = \Phi_2$) and either open or a power law boundary condition on the right (i.e. $\Phi_N/\Phi_{N-1} = \Phi_{N-1}/\Phi_{N-2}$).

Here we focus on the shell model defined in section 2.2. This model can be viewed as a particular implementation of the general model based on PV evolution introduced in [31] and re-derived in section 4 of this paper. The model can be run in ‘external shear flow version’ by turning off the zonal flow equation and setting $\bar{\Phi}_0 = \bar{\Phi}_{\text{ext}}$ or in ‘self-consistent zonal flows’ version, where the large scales are allowed to evolve dynamically, self-consistently with the small scales. It can also be driven in two different ways: The ‘instability drive version’ (i.e. $S_n = \gamma_n \Phi_n$) or ‘external drive version’ (i.e. $S_n = \Gamma_n$). In either case, γ_n or Γ_n are taken to be limited to only the first few (usually 2) shells.

Numerical results can be summarized as follows. First of all, we can clearly observe that the analytical solution (19) is reproduced by the numerical integration when the parameters are selected such that the interactions with the large scales dominate. The time evolution of this solution depends on model parameters and whether we use the external sheared flow version or the dynamic zonal flows version of the model. In the case of the external shear flow version, we see that the system simply evolves toward this fixed point, well represented by the analytical solution (see figure 4). In contrast, the dynamic zonal flows case provides rich dynamical behavior which can display predator–prey like oscillations (see figure 3), which may or may not be damped to a steady state (see figures 4 and 5) depending again on parameter values.

The observation of predator–prey like oscillations is in accord with the formulation presented in [34], and a similar phenomenon observed in gyrokinetic simulations [35] as a result of collisional damping of zonal flows. We note that the model damping at large scales (e.g. ν_F in equation (18)) plays the key role in setting the frequency and the amplitude of these inherently non-linear oscillations.

5.1. Predator–prey oscillations

A simple physical explanation for these oscillations can be suggested by studying the ‘minimum’ shell model with two-shells + the large scale mode. In this case the shell model reduces to a coupled set of three ordinary differential equations:

$$\frac{\partial \Phi_1}{\partial t} + \bar{\alpha}qgk \frac{(1 + g^2k^2 - q^2)}{(1 + k^2)} \bar{\Phi}^* \Phi_2 = \gamma \Phi_1, \quad (47)$$

$$\frac{\partial \Phi_2}{\partial t} - \bar{\alpha}qgk \frac{(1 + k^2 - q^2)}{(1 + g^2k^2)} \bar{\Phi} \Phi_1 = -\nu k^2 g^2 \Phi_2, \quad (48)$$

$$\frac{\partial q^2 \bar{\Phi}}{\partial t} = \bar{\alpha}qk^3 g(g^2 - 1) \Phi_1^* \Phi_2 - \nu_F q^2 \bar{\Phi}, \quad (49)$$

where $k \equiv k_1$. Note that while Φ_1 is being driven by the linear instability, Φ_2 is damped. Even though the physical meanings of the terms are different, the non-linear structures of the

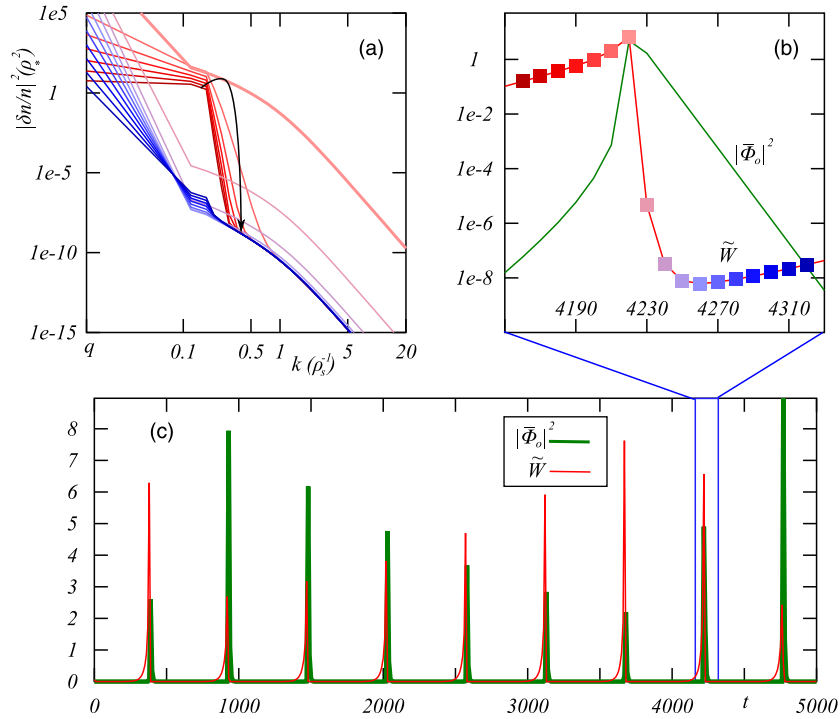


Figure 3. Spectral growth and collapse associated with predator–prey-like oscillations for the instability drive version with dynamic zonal flows case. The model parameters are $\alpha = 20$, $\bar{\alpha} = 10$, $\gamma = 4 \times 10^{-2}$, $\nu = 10^{-7}$, $\nu_{ZF} = 10^{-1}$ and $N = 54$. Here (a) shows the log versus log plot of k -spectra at different times, while (b) shows a log versus linear plot of time evolution of drift wave and zonal flow enstrophy and (c) is linear plot of drift wave and zonal flow enstrophies during the whole simulation. The color codes in (a) and (b) match, so that one can see that the time in (a) advances in the direction indicated by the arrow. The form of the spectrum during the oscillations agree perfectly with the analytical form $k^{-3}/(1+k^2)^2$.

equations are essentially the same with those of the three-wave interaction equations [36]. This kind of system is well known to display oscillation characteristics in multiple time scales. One common behavior is a relatively rapid oscillation between Φ_1 and Φ_2 (where the frequency is roughly proportional to $\bar{\Phi}$, which itself is modulated by these oscillations). At the same time $\bar{\Phi}$ acts as a slowly growing predator feeding on Φ_1 . As the level of $\bar{\Phi}$ increases, it takes more and more of the potential enstrophy of the Φ_1 and thus it depletes its own source of potential enstrophy. In the end it is the large scale damping ν_F , which reduces the large scale flow to a level where Φ_1 can grow again. This leads to the secondary oscillation. An example of the direct numerical integration of this two-shell model is shown in figure 6, where the large scale flow damping ν_F is varied as the main control parameter.

6. Results and conclusion

We have developed a number of shell models, which may be applicable to fusion plasma systems. Focusing on local interactions for strong turbulence and interactions with zonal flows and convective cells for weak turbulence limits, we believe that we cover a wide range of applicability. We started from a shell model based on local interactions for the simple

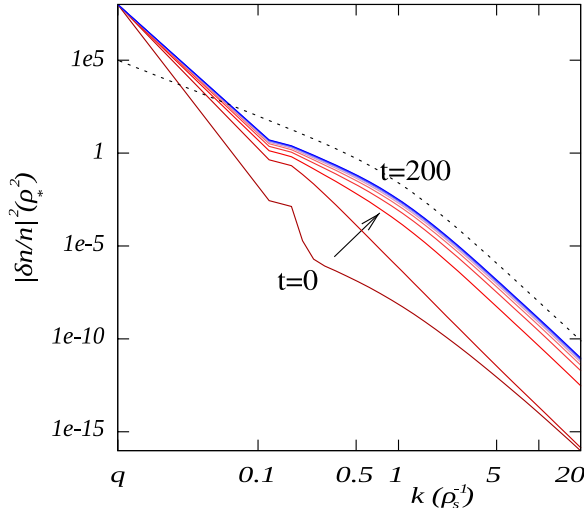


Figure 4. Spectral growth and saturation for the external drive version with external shear flow case with $\alpha = 20$, $\bar{\alpha} = 10$, $\Gamma = 1 \times 10^{-1}$, $\nu = 10^{-4}$ and $N = 44$.

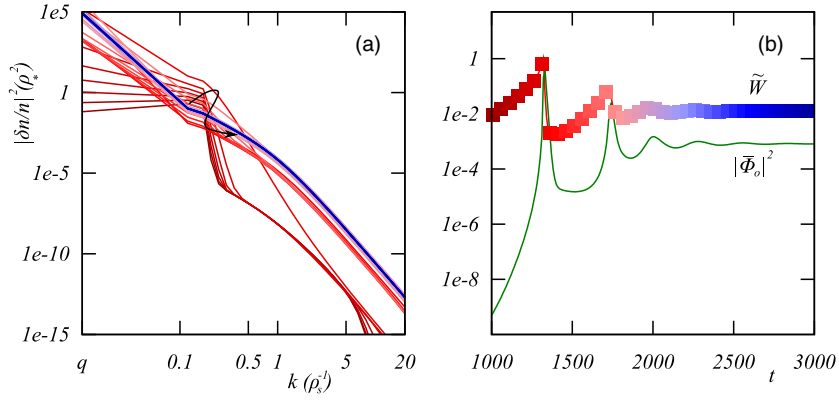


Figure 5. Spectral growth and saturation for the instability drive version with dynamic zonal flows, with $\alpha = 20$, $\bar{\alpha} = 10$, $\gamma = 10^{-2}$, $\nu = 10^{-6}$, $\nu_{ZF} = 10^{-1}$ and $N = 44$.

H–M system. Taking its continuum limit, we observed that it agrees well with the DAMs used for similar systems. Then, we included interactions with the zonal flows for a similar system which conserves PV. When disparate scale interactions with large scales dominate, we found a fluctuation spectrum of the form $|\tilde{n}_k|^2 \sim |\tilde{\Phi}_k|^2 \propto k^{-3}/(1+k^2)^2$ with the assumption of adiabatic electron response. We have further computed the continuum limit of this shell model, and verified that the part of the equation involving the interactions with the large scales had a form very similar to the wave-kinetic equation commonly used in weak turbulence formulation.

Furthermore, we developed a shell model for the two-field H–W system. We verified that all the standard 2D fluid spectra corresponding to velocity fluctuations (i.e. $|\tilde{\Phi}_k|^2 \propto \{k^{-14/3}, k^{-6}\}$) and passive scalars ($|\tilde{n}_k|^2 \propto \{k^{-8/3}, k^{-2}\}$) can be obtained as solutions to various limits of this H–W shell model. Finally, we generalized these observations in the form of a PV shell model, which is in principle applicable to any model that conserves PV. In general such models include drift instabilities such as ITG mode or models used on solar physics such as the β -plane MHD [37].

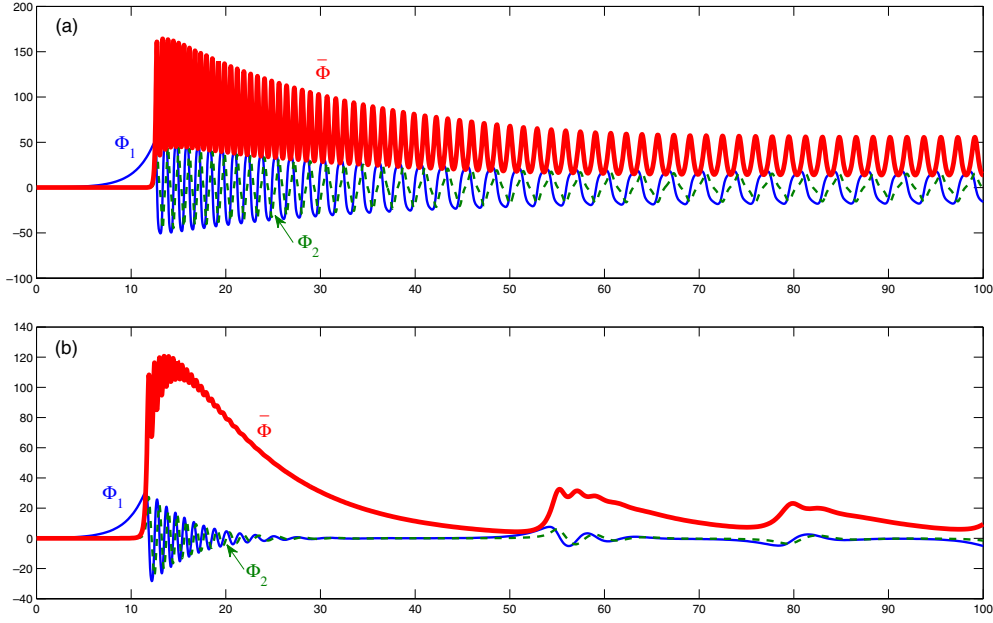


Figure 6. Predator–prey like oscillations observed in the reduced model with 2 shells and a large scale mode where the thin solid blue line is Φ_1 , the thin dashed green line is Φ_2 and the thick solid red line is $\bar{\Phi}$ (divided by 10 to represent in the same graph). The parameters are $g = 1.2$, $q = 0.01$, $k = 0.5$, $\bar{\alpha} = 1.0$, $\gamma = 0.5$, $\nu k^2 g^2 = 1.0$ and $\nu_F = 0.8$ for (a) and $\nu_F = 0.1$ for (b).

Acknowledgments

The authors would like to thank the organizers and participants of Festival de Théorie 2009 in Aix en Provence for valuable discussions. This work was carried out within the framework of the European Fusion Development Agreement and the French Research Federation for Fusion Studies (FR-FCM). It is supported by the European Communities under the contract of Association between Euratom and CEA. The views and opinions expressed herein do not necessarily reflect those of the European Commission. Financial support was also received from Agence Nationale de la Recherche ANR06-blan0084.

Appendix A. Continuum limit of the H–M system

Description of the continuum limit starts with a selection of a proper variable. The shell variable Φ_n scales with the square root of the shell area. Thus it makes sense to define instead a ‘shell averaged’ variable for the continuum limit by dividing the shell variable to the square root of the shell area:

$$\Phi(k_n) \equiv \frac{\Phi_n}{\sqrt{2\pi k_n \Delta k_n}},$$

where the shell width Δk_n is not constant. If we take $g = 1 + \epsilon$, we can see that $\Delta k_n = k_{n+1} - k_n = \epsilon k_n$. Inversely, we can write $\Phi_n = \epsilon^{1/2} k_n \Phi(k_n)$, which in the limit of small ϵ becomes $\Phi_n \rightarrow \epsilon^{1/2} k \Phi(k)$. The neighboring shell variables can be written using a Taylor expansion around k . For example,

$$\Phi_{n+1} = \epsilon^{1/2} k_{n+1} \Phi(k_{n+1}) = \epsilon^{1/2} k_n (1 + \epsilon) \Phi(k_n (1 + \epsilon)).$$

For simplicity, we define $f(k) = k\Phi(k)$ in terms of which we can expand each neighboring shell up to order ϵ^2 as

$$\begin{aligned}\Phi_{n+1} &\approx \epsilon^{1/2} \left[f(k) + \epsilon k f'(k) + \frac{\epsilon^2 k^2}{2} f''(k) \right], \\ \Phi_{n-1} &\approx \epsilon^{1/2} \left[f(k) - (\epsilon - \epsilon^2) k f'(k) + \frac{\epsilon^2 k^2}{2} f''(k) \right], \\ \Phi_{n+2} &\approx \epsilon^{1/2} [f(k) + (2\epsilon + \epsilon^2) k f'(k) + 2\epsilon^2 k^2 f''(k)], \\ \Phi_{n-2} &\approx \epsilon^{1/2} [f(k) - (2\epsilon - 3\epsilon^2) k f'(k) + 2\epsilon^2 k^2 f''(k)].\end{aligned}$$

Substituting these (and $g = 1 + \epsilon$) into (10) and re-arranging, we obtain

$$\begin{aligned}\epsilon^{1/2} \frac{\partial f(k)}{\partial t} &= \alpha \epsilon^2 \frac{k^4}{1+k^2} \left\{ (2 - 13\epsilon + 49\epsilon^2) \left[f(k)^2 - 3\epsilon k f(k) f'(k) \right. \right. \\ &\quad \left. \left. + \epsilon^2 \left(\frac{5}{2} k^2 f(k) f''(k) + 4k f(k) f'(k) + 2k^2 f'(k)^2 \right) \right] \right. \\ &\quad \left. - (4 - 6\epsilon + 10\epsilon^2) [f(k)^2 + \epsilon^2 (k^2 f''(k) f(k) - k^2 f'(k)^2 + k f(k) f'(k))] \right. \\ &\quad \left. + (2 + 7\epsilon + 9\epsilon^2) \left[f(k)^2 + 3\epsilon k f(k) f'(k) \right. \right. \\ &\quad \left. \left. + \epsilon^2 \left(\frac{5}{2} k^2 f''(k) + 2k^2 f'(k)^2 + k f(k) f'(k) \right) \right] \right\} \\ &= 6\alpha \epsilon^4 \frac{k^4}{1+k^2} [8f(k)^2 + 11k f(k) f'(k) + k^2 f(k) f''(k) + 2k^2 f'(k)^2]\end{aligned}$$

or in terms of $\Phi(k)$:

$$\epsilon^{1/2} k \frac{\partial \Phi(k)}{\partial t} = 6\alpha \epsilon^4 \frac{k^6}{1+k^2} [21\Phi(k)^2 + 17k\Phi(k)\Phi'(k) + k^2\Phi(k)\Phi''(k) + 2k^2\Phi'(k)^2]$$

which can be rearranged in the form of equation (12).

References

- [1] Mazzucato E 1976 *Phys. Rev. Lett.* **36** 792–4
- [2] McKee G *et al* 1999 *Rev. Sci. Instrum.* **70** 913–6
- [3] Zweben S *et al* 2004 *Nucl. Fusion* **44** 134–53
- [4] Hennequin P *et al* 2004 *Rev. Sci. Instrum.* **75** 3881–3
- [5] Kendl A, Scott B D, Ball R and Dewar R L 2003 *Phys. Plasmas* **10** 3684–91
- [6] Waltz R E, Candy J and Fahey M 2007 *Phys. Plasmas* **14** 056116
- [7] Casati A *et al* 2009 *Phys. Rev. Lett.* **102** 165005
- [8] Mator N and Diamond P H 1989 *Phys. Fluids B* **1** 1980–92
- [9] Hahm T S and Tang W M 1991 *Phys. Fluids B* **3** 989–99
- [10] Terry P W *et al* 2008 *Phys. Plasmas* **15** 062503
- [11] Kraichnan R H 1967 *Phys. Fluids* **10** 1417–23
- [12] Frisch U 1995 *Turbulence: The Legacy of A. N. Kolmogorov* (Cambridge: Cambridge University Press)
- [13] Coppi B, Rosenbluth M N and Sagdeev R Z 1967 *Phys. Fluids* **10** 582–7
- [14] Adam J C, Tang W M and Rutherford P H 1976 *Phys. Fluids* **19** 561–6
- [15] Horton W, Hong B G and Tang W M 1988 *Phys. Fluids* **31** 2971
- [16] Biferale L 2003 *Ann. Rev. Fluid Mech.* **35** 441–68

- [17] Diamond P H, Itoh S-I, Itoh K and Hahm T S 2005 *Plasma Phys. Control. Fusion* **47** R35–161
- [18] Hasegawa A and Mima K 1978 *Phys. Fluids* **21** 87–92
- [19] Ottinger J L and Carati D 1993 *Phys. Rev. E* **48** 2955–65
- [20] Yamada M and Ohkitani K 1988 *Prog. Theor. Phys.* **79** 1265–8
- [21] L'vov V S, Podivilov E, Pomyalov A, Procaccia I and Vandembroucq D 1998 *Phys. Rev. E* **58** 1811–22
- [22] Parisi G 1990 A mechanism for intermittency in a cascade model for turbulence *Preprint* University of Rome II, unpublished
- [23] Andersen K, Bohr T, Jensen M, Nielsen J and Olesen P 2000 *Physica D* **138** 44–62
- [24] Lilly D K 1989 *J. Atmos. Sci.* **46** 2026–30
- [25] L'vov V S and Nazarenko S 2006 *JETP Lett.* **83** 541–5
- [26] Sagdeev R Z, Shapiro V D and Shevchenko V I 1978 *JETP Lett.* **27** 340
- [27] Mattor N and Diamond P H 1994 *Phys. Plasmas* **1** 4002–13
- [28] Smolyakov A I, Diamond P H and Shevchenko V I 2000 *Phys. Plasmas* **7** 1349–51
- [29] Rhines P B and Young W R 1982 *J. Fluid Mech.* **122** 347–67
- [30] Diamond P H, Gürcan Ö D, Hahm T S, Miki K, Kosuga Y and Garbet X 2008 *Plasma Phys. Control. Fusion* **50** 124018
- [31] Gürcan Ö D, Garbet X, Hennequin P, Diamond P H, Casati A and Falchetto G L 2009 *Phys. Rev. Lett.* **102** 255002
- [32] Smolyakov A I, Diamond P H and Medvedev M V 2000 *Phys. Plasmas* **7** 3987–92
- [33] Galassi M *et al GNU Scientific Library Reference Manual (3rd Edn)* <http://www.gnu.org/software/gsl/>
- [34] Malkov M A, Diamond P H and Rosenbluth M N 2001 *Phys. Plasmas* **8** 5073–6
- [35] Lin Z, Hahm T S, Lee W W, Tang W M and Diamond P H 1999 *Phys. Rev. Lett.* **83** 3645–8
- [36] Kaup D J, Reiman A and Bers A 1979 *Rev. Mod. Phys.* **51** 275–309
- [37] Tobias S M, Diamond P H and Hughes D W 2007 *Astrophys. J. Lett.* **667** L113–6